Advancements in Drug Development and Formulation

Techniques for R&D, production, and analytical support

Dirk Leister
Leader, Technical Marketing Manager
Thermo Fisher Scientific

Ramesh Muttavarapu
Research & Development, Pharma Services Group
Thermo Fisher Scientific

Jennifer Empey
Applications Specialist, UV-Visible Spectroscopy
Thermo Fisher Scientific

Saurabh Mishra
Formulation Scientist/ Laboratory Manager
SE Tylose USA, Inc.

Margarethe Richter
Applications Specialist, Pharma
Thermo Fisher Scientific

Shaileshkumar Karavadra
Manager, Applications Scientist
Thermo Fisher Scientific

INTRODUCTION

A recent e-symposium presented insights into the latest research and innovative solutions to help shorten time-to-market, reduce development costs, increase yield, and assure quality and pharmacopoeia compliance throughout the drug development process. Useful strategies for oral solid dosage (OSD) formulation, drug delivery systems, and implant development were highlighted, as well as process R&D and manufacturing. The sessions covered several key techniques:

- Hot-melt extrusion for OSD and implants,
- Twin-screw granulation and continuous manufacturing,
- PAT for process monitoring and quality assurance,
- Raman microscopy for diagnosis and final product verification,
- and UV-Visible spectroscopy for quality control and adherence to pharmacopoeial standards.

HOT MELT EXTRUSION

Hot-Melt Extrusion for Pharmaceutical Applications: Dosage Forms, Process Insights, Product quality

Low solubility is a major issue for the development of pharmaceutical molecules. Of all the approved drugs in the last decades, more than half had poor solubility in water. Moreover, 29% of drugs in development fail preclinical trials due to low bioavailability. Dr. Margarethe Richter presented on the use of solid dispersions as one way to improve the solubility of molecules, as recommended because they are dispersed into fine particles.

The three types of solid dispersions comprise an amorphous (non-crystalline) polymer matrix with the active pharmaceutical ingredient (API) dispersed as crystals, amorphous particles, or dissolved in the polymer. From a thermodynamic point of view, the crystalline type is perfectly stable, the amorphous form is metastable (recrystallisation is kinetically controlled), and the solid glassy solution (dissolved API) is stable if the concentration stays below the saturation of the API in the polymer. Differential scaling calorimetry (DSC) can help to differentiate the types.

Hot-melt extrusion (HME), spray drying (SD), freeze drying, and supercritical fluid drying are different ways to prepare a solid dispersion. The most common are HME and spray drying. HME has several advantages over the other techniques. It is a solvent-free technology that eliminates the need to find a solvent suitable for the formulation as well as solvent handling. This results in a small production line. It is also dust free and continuous. With only a few processing steps, HME is highly reproducible and very easy to scale up at low cost. One of the important drawbacks of HME is the temperature at which it runs; not all drugs can handle the high temperature of the process.

HME combines thermal and mechanical energy to process polymeric materials above their glass transition temperature (Tg). Dry powder is fed into the system as a blend or split feed of the ingredients. The extruder has two parallel screws intermeshing and co-rotating in the same direction. The biggest advantage is that this technology mixes the materials on a molecular level. Once the melt is produced, it is pushed through a die for shaping. After, it is cooled down and sized. Various dosage forms can be produced with twin-screw processes: solid oral, transdermal, transmucosal, subcutaneous, and buccal. This versatility, along with the numerous advantages, explain why HME is so popular.

Downstream equipment is as important as the extrusion, itself, because it highly affects the shape of the product after extrusion. Some examples of typical downstream equipment used for the manufacturing of solid oral dosage forms (SOD) are strand line, face-cut pelletizer, chill roll, strand take-off, sheet take-off, and injection molding. The most commonly used are strand line, face cut pelletization, and chill roll. The first two generate pellets, while the third yields thin flakes that are easily milled. Sheet extrusion is recommended for making thin, orally dispersible films that readily dissolve in water. Subcutaneous implants are direct delivery systems that are also made using HME. They are typically shaped like thin, round extrudate or co-extrudate containing polymer material that can be biodegradable (dissolves in the body) or biodurable (compatible with the body but must eventually be removed).

The extruder helps monitor the HME process, as it collects all the data needed to check stability of the temperatures, pressure, torque, and feed rates. For continuous processes, constant process parameters lead to consistent product quality. In

addition to the extruder information, other online tools help determine the quality of the product. For example, the Thermo Scientific™ Antaris™ MX FT-NIR Spectrometer and iXR™ Raman Spectrometer from Thermo Fisher Scientific enable monitoring of the chemical composition of the extrudate.

Offline analyses are also useful for determining the quality of a final drug product. For example, a scanning electron microscope (SEM) can be used to examine the product surface, such as imaging an implant with the Thermo Scientific™ Phenom™ XL G2 Desktop Scanning Electron Microscope (SEM). This is important, as surface texture affects release of the drug. In addition, Raman mapping reveals the dispersion of the API in the product and can clearly reveal different co-extrudates (e.g., slow-release versus rapid-release polymers).

Twin-screw extrusion is a versatile technology, enabling R&D and production of different dosage forms and formulations on the same equipment. Using HME to produce a drug can significantly improve bioavailability. It is a well-established, continuous process with full GMP compliance. The machines are quite small, and disassembly and cleaning are very fast. In addition to easy scalability, the extruder is modular. Different applications/dosage forms are possible simply by changing accessories (up-/down-stream). The Thermo Fisher Scientific suite of extruders and analytical instrumentation cover a wide range of applications, from R&D to manufacturing.

Hot-Melt Extrusion: In-Process Monitoring and Final Product Verification

HME achieves a molecular level of mixing of the polymer and the active compounds to produce a finished product that meets the Target Product Profile (TPP) requirements. In addition to solubility enhancement, HME delivers a product that will remain stable throughout its shelf life. In-process monitoring ensures consistent quality of pellets, while downstream processing creates the final product that requires verification. Ramesh Muttavarapu presented on a recent case study that surveyed the entire process, including pellet production, downstream processing, process monitoring, testing, and final product verification.

The pelletization process from the study began with a gravimetric feeding mechanism that continuously and accurately fed powder to the extruder. Process data provides the feed rate, which must be kept uniform to achieve a high-quality product. The extrudate then enters the pelletizer, followed by the fluid bed cooler. After that, coating and encapsulation take place. In the case study, the pellets were split into two batches. One received an immediate release (IR) coating, while the other had a delayed release (DR) coating applied. The encapsulation step combined the IR and DR pellets to create bi-phasic release capsules. The process was very well controlled, with in-process monitoring of screw speed, throughput, extruder load, melt pressure, and temperature in 14 different zones. As shown in **FIGURE 1**, a very consistent, narrow pellet particle size range was achieved and confirmed by measurements at the beginning, middle, and end of the process. In addition, the coatings were very uniform, and the products exhibited a good drug release profile with no variability between the batches. Thus, the product met the TPP.

The production of controlled release tablets via an unconventional process has also been studied. In this approach, depicted in **FIGURE 2**, a blend is fed into an HME. Then, the strand that emerges goes through a cooling and cutting unit where it is cut into rods. The cut rods can then be compressed into tablets (or encapsulated). The temperature of the strand is critical for a smooth cut, so the optimal temperature must be determined and maintained.

The product content uniformity is based on the cut length and the weight of the cut rod. A weight check ensures that the individual units produced are within the specification range. This process is suitable for modified release tablets with 6 to 24-hour release requirements.

HME has proven to be a powerful and versatile tool for modern pharmaceutical formulation development. HME can be used for many applications, from increasing bioavailability to devising novel drug delivery methods. Thermo Fisher Scientific offers HME units appropriate for various batch sizes.

FIGURE 1: Pellets particle size (measured at beginning, middle, and end of the process).

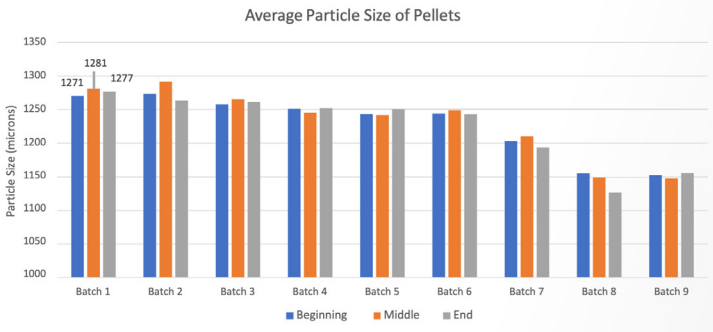

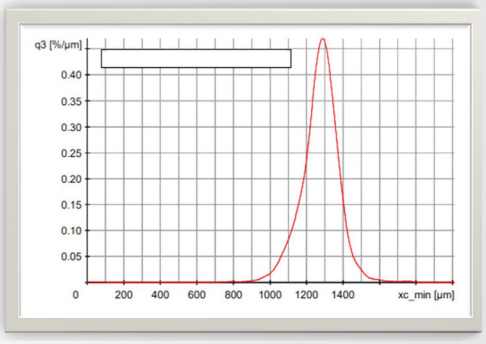

Very consistent and a narrow particle size range
Sieve cut fraction loss is very minimal
Very uniform coating
Good drug release profile (with no variability between the batches)

FIGURE 2: Hot-melt extrusion and strand cutting and compression.

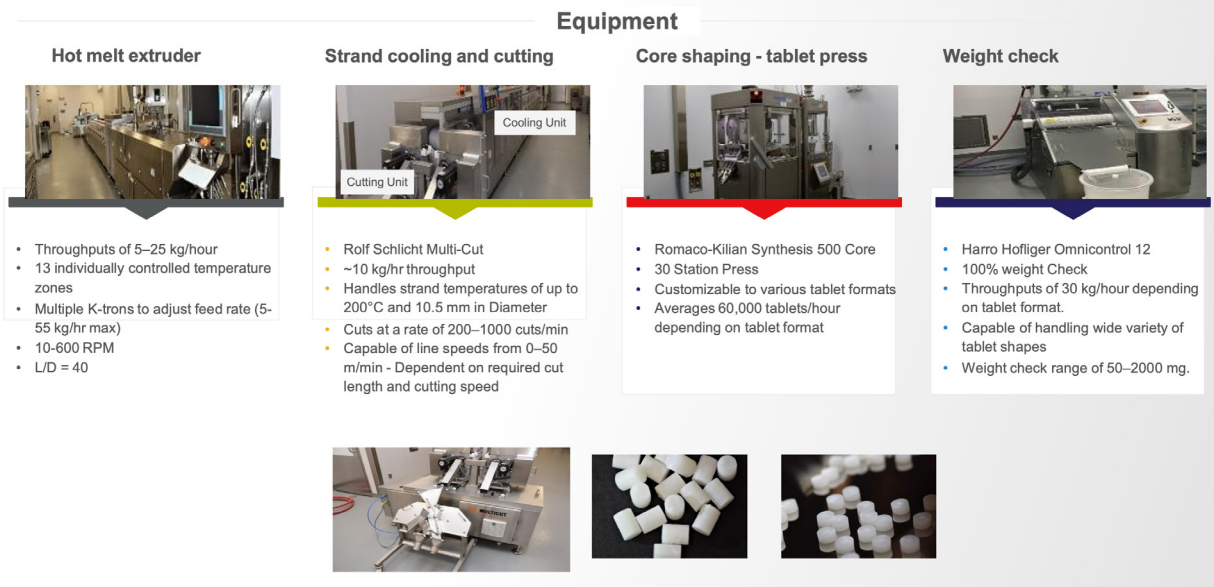

DOWNSTREAM PROCESSING

Downstream Processing of Itraconazole

HPMCAS Amorphous Solid Dispersion: From Hot-Melt Extrudate to Tablet Using a Quality by Design Approach

HME-based amorphous solid dispersion (ASD) offers many advantages, but further processing of the extrudates can be challenging. Saurabh Mishra discussed the utilization of a robust platform for downstream processing that was established using a quality by design (QbD) approach.

Different cutting techniques at the end of the extruder barrel and different milling conditions were tested for their influence on critical quality attributes (CQAs). For a successful scale-up, correlations from early-formulation hand-cut processing at the lab scale to industrial-sized processes have been established.

Downstream processing is commonly carried out by hand-cutting extrudates and milling, then further sieving, as per desired particle size. This limits its application for industrial aspects involving large scale production. Thus, a robust platform for downstream processing of HME-based amorphous solid dispersions relevant for lab scale up to production scale is required.

A recent study compared three different processing methods of HME extrudates based on an ASD of poorly soluble itraconazole (ITZ) with a medium substitution and particle size grade of hypromellose acetate succinate (HPMCAS-MMP) as a carrier polymer. To prepare the ASD, ITZ and HPMCAS-MMP (20:80) were blended in a tubular mixer for 15 minutes and hot melt extruded at 165°C using a twin-screw extruder with three mixing zones. For hand-cut premilled (HCF) feedstocks, the blend was extruded, hand-cut, and milled using a hammer mill. Preparation of pellet (PE) feedstocks involved the extrusion followed by cooling and palletization with a Varicut pelletizer. To prepare chill roll flakes (CRF) feedstocks, the blend was extruded, passed through a chill roll, and flakes were formed.

A customized Response Surface Methodology was derived, for which the feedstocks were subjected to varying milling speeds and mesh sizes in a series of 18 experiments. Milling was carried out on 100 g of feedstock and hammer milling for 90 seconds. Several critical quality attributes (CQAs) were then evaluated, including milled granules yield (%), milled granules D50 (volume mean particle size in µm), tablet tensile strength (MPa), tablet dissolution Q30 (ITZ release in 30 minutes), and tablet dissolution Q60 (ITZ release in 60 minutes). The first CQA was calculated by weight, while the D50 was measured by a laser diffraction method (Helos & Rodos). The curved face equation was used to calculate the tablet tensile strength. High-performance liquid chromatography (HPLC) provided Q30 and Q60 values. Further evaluation applied a polynomial quadratic equation to study the quadratic effects as well as the interaction effects: $Y=B_0+B_1X_1+B_2X_2+B_3X_3+B_{12}X_1X_2+B_{23}X_2X_3+B_{13}X_1X_3+B_{22}X_2^2+B_{33}X_3^2$. Y is the predicted or measured response, B_0 is the model constant or intercept, and X_1, X_2 and X_3 are independent variables feedstock, milling speed and mesh diameter. B_1, B_2 and B_3 are linear coefficients, while B_{12}, B_{23} and B_{13} are interaction terms or cross-product coefficients, and B_{11}, B_{22} and B_{33} are quadratic coefficients.

A preliminary trial was performed to determine the maximum load. For this trial, hand-cut filaments were milled at three different RPMs to obtain three different particle sizes. They were then compacted into three different ASD loading fractions and the tensile strength was evaluated. The maximum of 50% ASD loading at all the milling conditions was achieved, revealing

tensile strength more than 1.7 MPa.[1] Thus, 50% ASD loading was selected for further formulation development.

To make the tablets, powder blends were compacted using an 11.5 mm round biconvex punch at a compression load of 20 kN. Tablets were compacted at 650 mg, consisting of a 65 mg dose of Itraconazole to be equivalent to the brand product, Tolusra® capsules. For compaction analysis, all three feedstocks (HCF, PE, and CRF) were milled at 5000 RPM and 15000 RPM using 1 mm mesh. Tablets were compacted at 50% ASD load at different compression loads (25-250 kN) and tabletability, compressibility and compactibility was evaluated.[2]

Images of the feedstocks revealed that PE appears as ordered cylinders, whereas HCF and CRF exhibited irregular shapes. When preparing feedstocks, there is always concern that the drug will be converted to its crystalline form. In this study, DSC and powder X-ray Diffraction (PXRD) confirmed that the ITZ remained amorphous in all three feedstocks. The effect of the independent variables as per the experimental design using the customized response surface methodology assessed the impact of milling speed and mesh size on yield. It was found that HCF and CRF showed an increase in percent yield, while the PE had a significantly decreased yield. This is likely due to the ordered cylindrical shape of the PE, as milling occurs at the plane of the pellets. In comparison, the irregular shapes of the HCF and CRF cause them to contain internal weaknesses. Understandably, increases in milling speed and mesh size increased the yield.

Regarding the effect of the independent variables on particle size distribution (PSD), CRF yielded a small distribution while HCF's was somewhat larger. PE showed a much higher PSD and D50 value than the other feedstocks. The low PSD of CRF could be due to its irregular shape, or its large surface area after exiting the roller. Alternatively, it may relate to its cooling rate, which inhibits structural relaxation. This leads to reduced elasticity of the extrudate so that there is greater size reduction during milling. As one would expect, increasing the milling speed decreased the D50 values, whereas increasing the mesh size increased them.

Further exploration of the effect of feedstocks on PSD produced interesting results, as shown in **FIGURE 3**. The three

FIGURE 3: Effect of feed stocks on particle size distribution.

- To study the effect of different ASD feedstocks (HCF, PE, CRF) were milled at two different milling speed of 5000 rpm and 15000 rpm using 1 mm mesh
- Monomodal size distribution could be observed for the milled ASD extrudates at both 5000 and 15000 rpm with 1.0 mm sieve.

Type of Feedstock	Milled at 5000 rpm, 1 mm mesh			Milled at 15000 rpm, 1 mm mesh		
	D10(µm)	D50 (µm)	D90 (µm)	D10 (µm)	D50 (µm)	D90 (µm)
HCF	197.59	436.02	753.22	162.49	259.72	501.2
PE	227.53	517.48	840.90	118.69	259.65	491.75
CRF	177.3	420.69	743.83	70.03	178.68	376.58

- At lower milling speed of 5000 rpm, HCF and CRF feedstock almost similar PSD and at higher milling speed, PE shows almost similar PSD with HCF.
- Thus, with varying milling speed and same mesh size, correlation between PSD of all three feed stocks (HCF, PE, CRF) can be established.

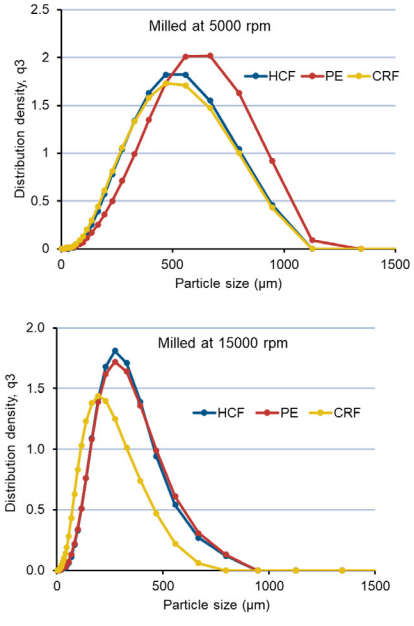

feedstocks were milled at two different milling speeds, 5000 RPM and 15000 RPM, using 1 mm mesh. At the lower milling speed, HCF and CRF feedstock had very similar PSDs, while PE's was very different. However, at the higher milling speed, PE showed a very similar PSD with HCF, but CRF's distribution differed considerably. Thus, with varying milling speed and the same mesh size, a correlation between PSDs of all three feedstocks can be established.

Moreover, all feedstocks had a significant effect on the tensile strength. HCF and PE had lower values; however, CRF had significantly higher tensile strength. This makes sense, as lower particle size distributions correlate to higher tensile strength. Accordingly, higher tensile strength can be achieved with higher milling speed, as it leads to smaller particle sizes. Larger mesh size will result in lower tensile strength. To assess the significance of PSD of milled ASD extrudates on tensile strength, a Pearson correlation coefficient test was conducted. A significant relationship was found between D50 and tensile strength, indicating that an increase in D50 causes significant decrease in tensile strength of the tablet.

Among the feedstocks, CRF showed the lowest PSD, so that tensile strength was higher due to its higher bonding surface area and bonding strength compared to HCF and PE.

For compaction analysis of the milled feedstocks, determining the tabletability, compressibility, and compactibility profile of the powders milled at 5000 RPM and 15000 RPM led to understanding the mechanics of tablet formation. Tabletability is a measure of tensile strength as a function of compression pressure. Solid fraction as a function of compression pressure determines compressibility, and solid fraction as a function of tensile strength defines compactibility. CRF showed higher tabletability and compactibility compared to PE and HCF. This is likely due to its lower PSD and resulting higher tensile strength. This result indicates that particle size distribution is the most important parameter. Interestingly, compressibility was the same for all three feedstocks irrespective of their different PSDs.

Evaluation of the ITZ dissolution is shown in **FIGURE 4**. The Effect chart indicates that the CRF feedstock delivered much higher Q30 and Q60 compared to HCF and PE. This relates

FIGURE 4: Effect of independent variables on dissolution of ITZ.

Fitting parameters	Q30(µg/mL)	Q60(µg/mL)
R^2	0.9314	0.9293
Adj. R^2	0.8056	0.7997
Root Mean Square Error (RMSE)	3.97	3.09
Mean of Response	37.90	46.35
Observations (or Sum Wgts)	18	18

$$Q30((\mu g/mL)) = 36.01 - 4.15X_1[HCP]^* - 3.59X_1[PE]^* + 7.75X_1[CRF]^* + 5.99X_2^* - 3.60X_3$$

$$Q60(\mu g/mL) = 44.73 - 2.05X_1[HCP] - 2.80X_1[PE]^* + 4.85X_1[CRF]^* + 4.68X_2^* - 2.73X_3$$

Here X_1, X_2 and , X_3 is feedstock, milling speed and mesh size respectively.*Only significant coefficients from quadratic and interaction term has been shown in the equation

↑ Milling speed = ↑ Q30 and Q60; ↑ Mesh size = ↓ Q30 and Q60

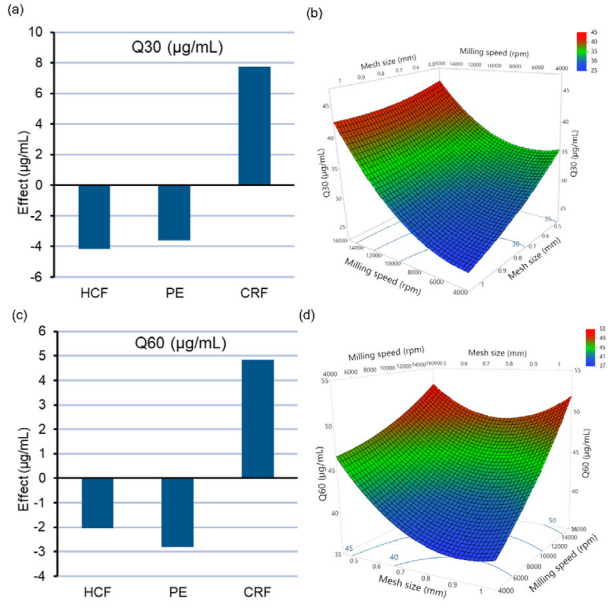

to its lower PSD. The Response plot bolsters this reasoning, as it reveals that higher milling speeds, which cause smaller particle sizes, lead to better dissolution. Similarly, larger mesh sizes correlate to lower Q30 and Q60 values. To further understand the importance of PSD on dissolution, a Pearson correlation coefficient test assessed D50's correlation with Q30 and Q60. A strong negative correlation was observed for both dissolution values, which indicated that lower D50 of milled extrudates causes higher dissolution of ITZ from the ASD tablet. This finding reinforces the results of the Effect and Response plots, as CRF showed the lowest PSD, and its dissolution of ITZ (Q30 and Q60) was found to be higher compared to HCF and PE. The drug release plots in **FIGURE 5** illustrate the relationship of milling speeds with the amount and rate of drug release. Clearly, CRF releases more ITZ in both graphs. The left plot demonstrates that at a milling speed of 5000 RPM, Q30 and Q60 are correlated with PSD of the feedstocks. However, at that milling speed, CRF and HCF have similar PSDs, yet the graph shows that higher supersaturation is achieved by the CRF feedstock. At the higher milling speed of 15000 RPM, dissolution and supersaturation of ITZ was found to be PSD dependent, with CRF feedstocks showing the fastest release of ITZ with instant supersaturation compared to HCF and PE.

This study illustrated the challenges of downstream processing of HME extrudates, including sizing milling and tableting. Using an ASD of poorly soluble itraconazole with hypromellose acetate succinate carrier polymer, it was found that after careful selection of milling speed a similar PSD was observed from the milling of hand-cut filaments in comparison with the milling of pellets or chill roll flakes.

This demonstrated the possibility of an easy transfer from early-formulation hand-cut processing at the lab scale to industrial-applicable processes. Among the feedstocks, the highest percentage yield with a lower PSD was observed for chill roll flakes compared to hand-cut filaments and pellets. The tensile strength and ITZ release from ASD tablets were also found to be the highest after the milling of chill roll flake feedstock, thereby indicating PSD as most important CQA of milled extrudates.

FIGURE 5: Effect of feed stocks on dissolution of drug.

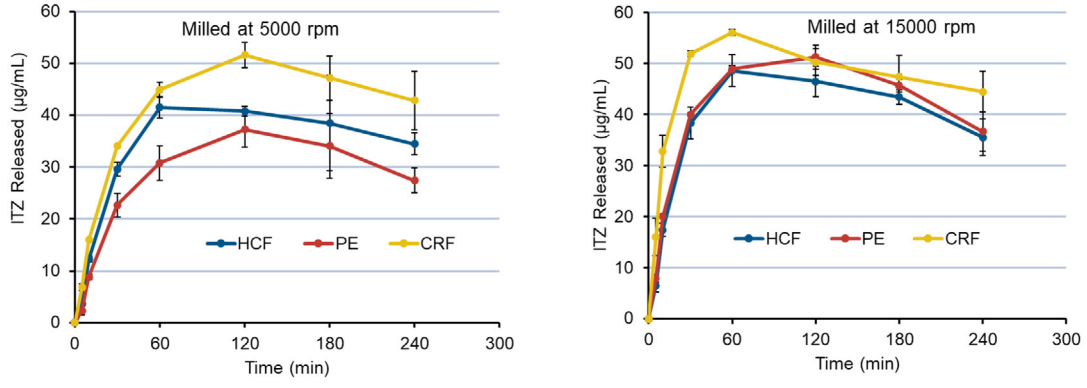

- At milling speed of 5000 rpm Q30 (µg/mL) and Q60 (µg/mL) is correlated with PSD of feedstocks
- However, higher supersaturation is achieved by CRF feedstock compared to HCF despite having almost similar PSD.
- Whereas in case of higher milling speed of 15000 rpm, Q30, Q60 and supersaturation of ITZ was found to be PSD dependent with CRF feedstocks showing fastest release of ITZ with instant supersaturation compared to HCF and PE

GRANULATION AND PAT MONITORING

Introduction to Twin-Screw Processes for Pharmaceutical Applications: TSG

Continuous granulation offers opportunities to overcome several challenges of traditional batch production of tablets and capsules. As presented by Dirk Leister, the technique is both efficient and inherently scalable, advancing to a point of true reliability and flexibility. It can also be implemented all at once, or a little at a time.

Twin-screw applications can be divided into two different processes: with a die (extrusion) and without a die (granulation). Extrusion can be performed by heating a polymer in hot-melt extrusion or by using a liquid binder for wet extrusion. In contrast, granulation can use a thermoplastic binder for dry/heat-activated granulation or use a liquid binder for wet granulation. The benefits of granulation, an agglomeration process that increases mean particle size, are numerous. It decreases the specific surface area and increases the bulk density. Importantly, it leads to better flowability for dosing and feeding while avoiding segregation and producing less dust. Granulation also makes compaction easier in tablet pressing (or makes compaction possible at all). The granules can be used directly for oral applications or in the compaction process to form a tablet.

The process for wet twin-screw granulation (TSG) typically takes place at room temperature. A powder or blend of powders is fed into an extruder barrel, and a binder liquid is added via an adjacent feed. With no die at the end of the barrel, there is no pressure. Rotation of the screws induces shear energy that causes agglomeration of the particles. Free flowing granules then leave the system through an open discharge. With high moisture content, the granules can be directly conveyed into a drying system before tableting. Process analytical technology (PAT) can vary from visual inspection to spectroscopic applications.

A recent case study for continuous wet granulation employed the combination of a Thermo Scientific™ Pharma 11 twin-screw system and a Glatt® MODCOS XS-Line (modular continuous granulation system) with a fluid bed dryer. A solid pre-blend placebo formulation comprising 5% Polyvinylpyrrolidone (PVP) 30, 32% corn starch, 62.8% lactose, and 0.2% talcum was combined with water for the granulation. PAT incorporated the direct imaging particle size Analyser Eyecon$_2$™ from Innophama Technology for particle characterization. The influence of the process parameters on the granule quality was analyzed, including throughput, liquid to solid (L/S) ratio, screw speed, barrel temperature, and screw configuration.

The benefits of granulation, an agglomeration process that increases mean particle size, are numerous.

It was found that increasing the L/S ratio caused the granules to become larger. More oversized particles were produced, there were fewer fine particles, and the density of the granules increased. This is typical for wet granulation techniques. The influence of screw speed was also of interest. **FIGURE 6** shows the impact of

increasing the screw speed at a fixed L/S ratio of 0.25. The left graph illustrates that as the screw speed is increased step-wise from 300 RPM to 900 RPM, the average particle size decreases. This is due to much more shear energy being introduced into the system. Moreover, the particle size distribution becomes narrower, as evidenced by the increasing slopes of the curves at higher rpms. Narrowing PSD as a function of increasing screw speed is also demonstrated in the graph on the right.

The intensification of mixing is another important parameter, as it can be used to tailor the properties of the granules. Different screw elements create different shear in the system; kneading elements offer high shear properties. To increase the intensification of mixing, the number of kneading elements on the screw shaft can be increased, or the offset angle between the individual mixing elements can be raised. The result will increase the filling level of the extruder and lead to higher compaction of the material. The D50 and number of oversized particles in the system will rise, as will the density of the obtained granules.

Continuous granulation offers several advantages over batch processes. It can save up to 80% of time and materials for research and development. Batches require repeated startups, stabilization, shutdowns, and cleaning in between, which are not necessary with a continuous process. Monitoring parameters and making changes can occur in a continuous process without the need to stop running. This allows quick reactions on demand, less waste, and more consistent quality. Less storage is needed as well. Handling errors are reduced, meaning there is less material "at risk." In addition, the use

FIGURE 6: Increasing screw speed.

Particle size distribution	$D_{v,50}$	Oversize Particles	Fines	Density of Granules
-	-	-	0	

[Thompson2010]

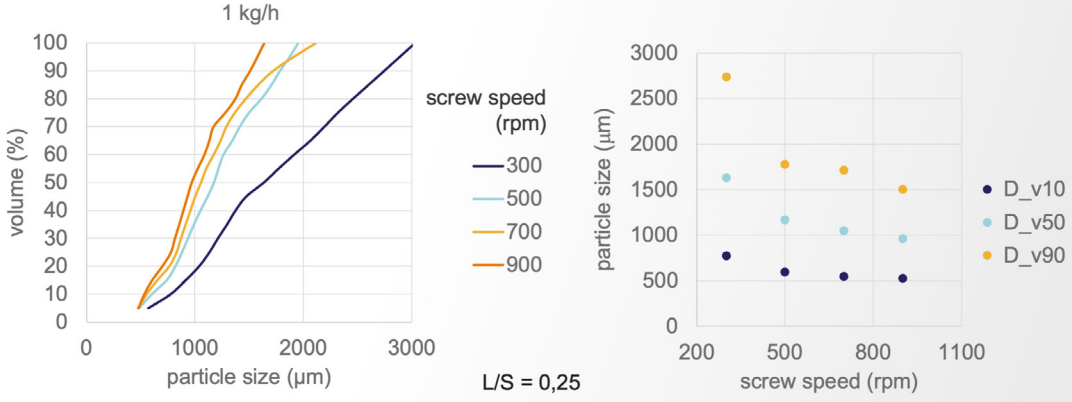

of PAT minimizes the production of unacceptable product. A constant process means constant product quality.

For scale-up of continuous granulation, granules from the Pharma 11 and benchtop Glatt MODCOS XS-Line continuous granulation system were compared to those from the Pharma 16 and production scale Glatt MODCOS S/M-Line. The graph in **FIGURE 7** demonstrates successful scale-up, as the particle size distributions for the small scale and production scale systems are nearly identical.

Well comparable to other granulation technologies, twin-screw granulation is a versatile technology that allows the tailoring of granule properties based on process parameters. Continuous TSG offers several benefits over batch production due to time and material savings, flexibility, and consistent quality. It has also been shown that granule quality produced on a small scale is predictive for granule quality obtained on a larger scale.

FIGURE 7: Scale-up continuous granulation.

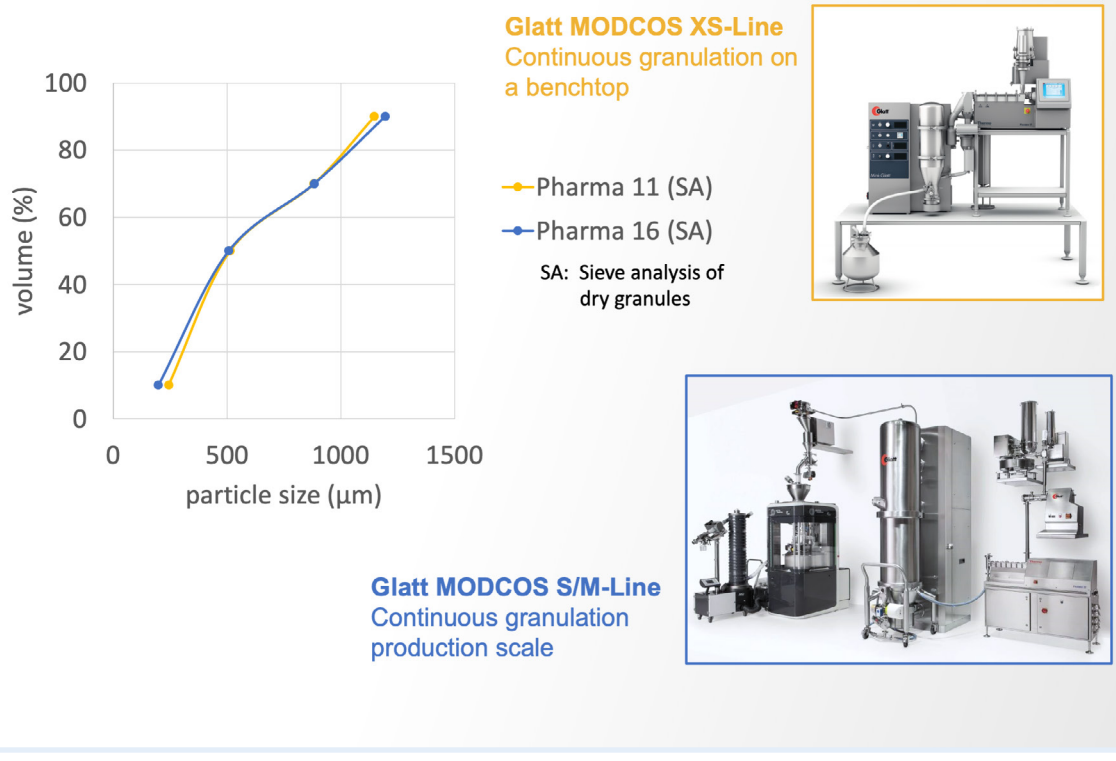

Granulation and PAT for Monitoring Granulation

TSG is greatly affected by variation within raw materials. Shaileshkumar Karavadra presented on the use of vibrational spectroscopy analytical techniques for monitoring granulation as well as for quality control testing of final products.

Vibrational spectroscopy is commonly employed to detect differences within and between raw material batches, monitoring API and excipient variability, and evaluating crystallinity, hydration, and polymorphism. For PAT solutions, vibrational spectroscopy monitors CQAs, blend homogeneity, API concentration, moisture and drying. Distribution of the API and binder, dissolution chemical imaging, foreign particle identification, and confocal coating analysis are just a few of the contributions of vibrational spectroscopy to QC testing of the final product. Highlighted features of the Thermo Scientific™ Nicolet™ iS50 FTIR Spectrometer, which offers Fourier-transform infrared spectroscopy (FTIR), Fourier transform near-infrared spectroscopy (FT-NIR), and Fourier transform Raman spectroscopy (FT-Raman) in one instrument. The Thermo Scientific™ DXR3xi Raman Imaging Microscope and Nicolet RaptIR™ Infrared Microscope deliver advanced imaging capabilities and ease of use for rapid answers in support of a myriad of applications.

Raman spectroscopy is an inelastic scattering phenomenon that probes molecular vibrations to provide a molecular fingerprint of materials. FTIR is a form of vibrational spectroscopy that relies on the absorbance, transmittance, or reflectance of infrared light. Using this method, light is absorbed in different amounts in a sample at distinct frequencies which correspond to the vibrational frequencies of the bonds in the sample. Raman and FTIR spectroscopy differ in some key fundamental ways. Raman spectroscopy depends on a change in polarizability of a molecule, whereas IR spectroscopy depends on a change in the dipole moment. Raman spectroscopy measures relative frequencies at which a sample scatters radiation, unlike IR spectroscopy which measures absolute frequencies at which a sample absorbs radiation. FTIR is sensitive to hetero-nuclear functional group vibrations and polar bonds, especially OH stretching in water. Raman, on the other hand, is sensitive to homo-nuclear molecular bonds. For example, it can distinguish between C-C, C=C and C≡C bonds.

Both methods can be used with microscopic techniques. The primary advantage of Raman spectroscopy is that it requires little to no sample preparation while the FTIR method has constraints on sample thickness, uniformity, and dilution to avoid saturation. The key advantage to FTIR is its ability to deal with interference: fluorescence may interfere with the ability of taking Raman spectra, which would not be an issue with FTIR. While both methods have advantages and limitations, the combination of these two methods becomes a powerful tool when performing materials characterization.

Process Raman is extremely useful for monitoring wet granulation processes. Wet granulation is the method of choice when large-dose drugs are to be compressed, as it delivers improved compressibility of powders and ensures better content uniformity, especially for soluble low-dose drugs. However, when a wet granulation is performed using shear energy, it may affect the components, thereby compromising therapeutic efficacy. Therefore, the components should be monitored for changes in their molecular structure. Determining the spatial distribution of the particles and checking for impurities and defects is also advised. PAT using Raman spectroscopy is ideal for these applications.

Continuous manufacturing requires the production process to be well controlled in its steady state. Thorough understanding of critical process parameters can be achieved with continuous monitoring.

Controllable process variables include the speed of material flow, extrusion temperature, distribution profile, and screw speed. The advantages of using Raman for PAT are numerous. It is non-contact, non-destructive, and is not susceptible to moisture. In addition, its selectivity and sensitivity are higher than NIR. Raman is an incisive, responsive, and comprehensive process indicator for product quality control.

A recent case study involving theophylline response to humidity monitored API quantification during wet granulation using Raman provides an example of a PAT application. The results are shown in **FIGURE 8** with spectra of the reference and standards highlighted in the upper left of the figure. A second derivative is typically applied to increase the resolution and reduce background. Note that the calibration required only five samples, whereas NIR would have demanded far more due to its lower sensitivity and resolution. The bottom graph in the figure signals the respiratory drug's gradual partial conversion to hydrate form with exposure to humidity. This information demonstrates Raman spectroscopy's value for controlling wet granulation processes.

In-line FT-NIR is also very useful for granulation monitoring. Near infrared spectroscopy can monitor not only the chemical changes of the sample but the physical properties of the matrix or extrudate. For example, it can monitor the change in particle size, the moisture, the water activity, and the percentage of API. This saves time by avoiding off-line testing and by providing immediate results that can be used to actively control the extrusion process and complete the control loop. There are probes for reflection (opaque) or transmission (clear) sampling. Real-time FT-NIR analysis offers several benefits. It reduces the amount of laboratory analyses and decreases labor costs as it reduces the frequency of manual sample extraction. Moreover, it lowers

FIGURE 8: API quantification during wet granulation using Raman.

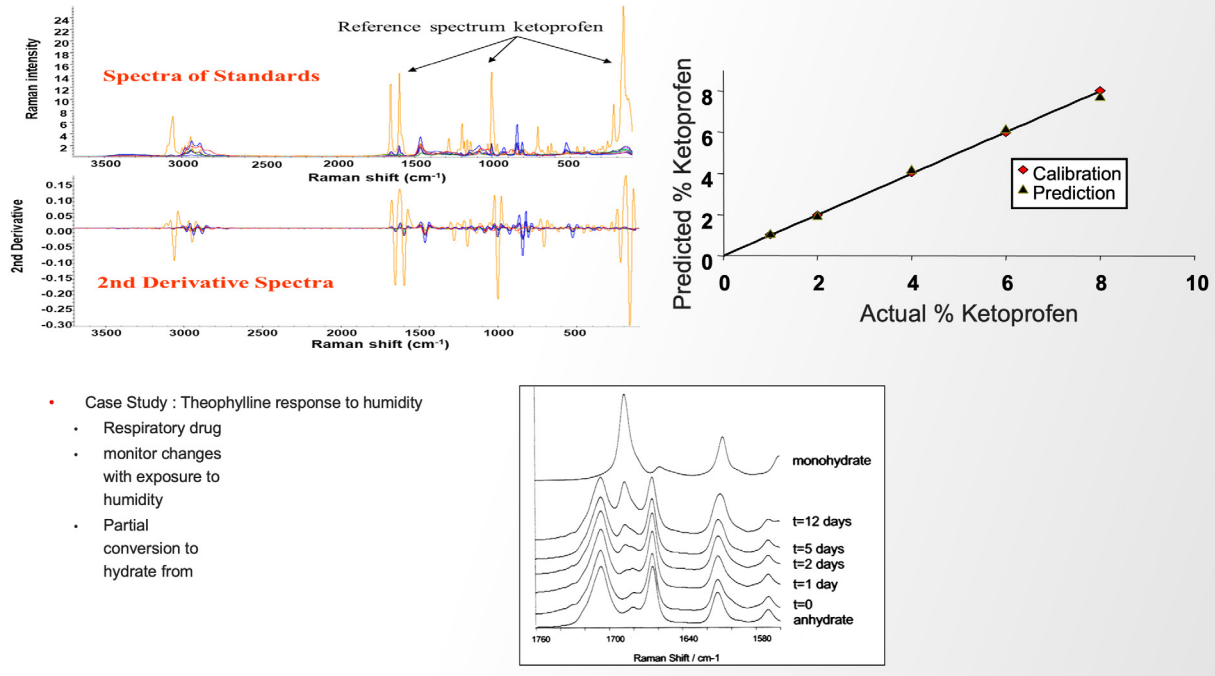

the risk of losing batches due to over drying. This can be significant, as $5500/kg material in a 150 L reactor would be valued at $825,000 (USD) per batch. The analysis provides "real-time" status of the drying process and automated feedback for blending or tablet production optimization. The near infrared light can be routed through long lengths of fiber optic cable so the system can sit in a safe, remote location. Fiber optic sampling features an air purge on the optical window, which avoids optical fouling as well as a retractable probe with automatic cleaning for wet and/or sticky samples.

An example of using a NIR fiber optic reflectance probe during fluid bed drying is shown in **FIGURE 9**. The wavenumbers ranged from 10,000 cm^{-1} to 4000 cm^{-1} and the water peaks are clearly visible in the large plot. Moisture content ranged from 2% to 25%. NIR can be used to monitor the moisture content within the sample or the endpoint of drying, as shown in the plot on the lower right of the figure. It also provides the water activity of the sample and, sometimes, even the bound and free water applications within the TSG.

Many issues from the field of pharmaceutical and medical R&D require the use of surface analytical techniques. Examples include residues and contamination in ampoules, particles in and discoloration of blister packaging, residues from cleaning agents in syringes and needles, the distribution of APIs on stents, implants or patches, delamination of coatings, and many more. The drug form (galenic form) can also be the subject of surface analysis. Raman microscopy provides identification of the different molecules of API and excipients. With Raman imaging, the dosage form and the API distribution can be shown in a detailed map of the tablet. The layer structure can be examined confocally for a depth profile as well.

Semi-quantitative information can be obtained in finished tablet imaging when concentrations of ingredients are

FIGURE 9: Fluid bed drying: calibration for endpoint detection.

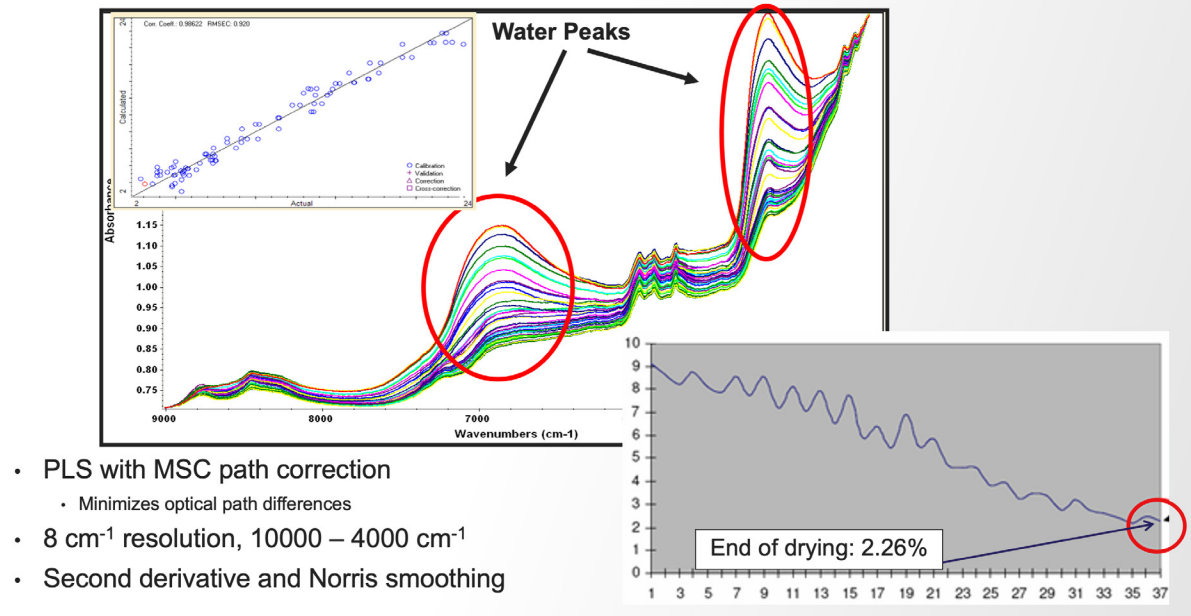

unknown by using multivariate curve resolution (MCR). The distribution and approximate quantifications of the API and excipient are measured in minutes. Calibration is not required; the raw materials can be used to create a library that allows the correlation plot for the active and excipient concentrations to be calculated in real time using MCR.

The entire surface area of a 3-active component tablet was analyzed. Shown in **FIGURE 10**, the surface area was 11 mm x 11 mm, and the image comprises 226,000 spectra with 25µm spectrum spacing. The spectra were acquired at 550 Hz (1.8 ms/spectrum) for a total collection time of only 8 minutes. The entire surface of the tablet was quickly analyzed to determine domain size, distribution of the domains, and composition. A subsequent three-hour high-resolution collection used smaller step size and faster scanning speed. This revealed the presence of low Raman scattering excipients starch, cellulose, and sodium lauryl sulfate. This analysis had a 0.5 mm pixel size and 100 Hz (10 ms/spectrum) acquisition rate. The ability to use such high resolution makes it possible to analyze for any type of compound present: active ingredients, binders, and contaminants.

FIGURE 10: Surface analysis of an entire headache tablet.

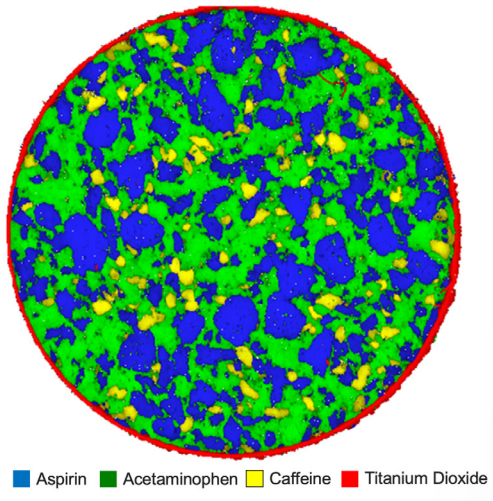

Determine:
•Size of each domain
•Distribution of domains
•Overall composition of tablet

11 x 11 mm surface area
532 nm laser, 10X objective

226,000 spectra, 25 µm pixel size

Acquisition parameters: 550 Hz (1.8 ms/spectrum)

8 minute collect time!!

IMPLANTS AND APPLICATIONS OF VIBRATIONAL SPECTROSCOPY

Introduction to Twin-Screw Processes for Pharmaceutical Applications: Implants

Subcutaneous implants are drug delivery systems consisting of a polymer loaded with an API. They can be produced by hot-melt extrusion and are typically thin, round extrudate, or co-extrudate. The polymer material can be biodegradable, which dissolves over time, or biodurable, meaning it must be removed after a specified period of time. As presented by Dirk Leister, injectable implants are widely applicable and offer numerous benefits:

- Site-specific controlled release of therapeutic agents – lower drug dose needed, fewer side effects
- Increased patient compliance – no scheduled pill intake (good for elderly patients)
- Potent drug delivery – hormones, opioids, antibiotics, oncology drugs
- Wide range of indications - treatment of schizophrenia, cancer, ophthalmology, contraception

Implant research and development is simplified with the Thermo Scientific Pharma mini HME, a conical micro compounder for hot-melt extrusion. This very small twin-screw extruder ensures a stable process with constant pressure and torque at a very low throughput rate, which has been proven ideal for implants. Its maximum temperature of 280°C allows processing of a wide range of polymers. The screws can be co-rotating or counter rotating. The latter produces a pumping effect with high-pressure extrusion and narrower residence time distribution. In contrast, co-rotating screws have a twin-screw mixing effect with low-pressure extrusion and wider residence time distribution, which is preferred for implant HME. A Thermo Scientific™ CaliCut Post-extrusion system interfaces with the Pharma mini HME and calibrates and cuts the extruded strand into the desired final form of the implant. The diameter of the strand is measured with a laser gauging system that has a feedback loop to the belt speed. The hot polymer strand can be stretched or compressed by varying the belt speed, leading to a very uniform strand diameter throughout the process. This is critical, as only the precise diameter ensures the desired API concentration in the implant. Different sized belts and cutting mechanisms are available.

An example of a contraceptive implant is shown in **FIGURE 11**. For this application, an inner core of ethylene-vinyl acetate (EVA) with the API is co-extruded through a specialized die with an EVA outer membrane. The membrane's function is to control diffusion of the API over a three-year period. The qualitative concentration-time profile indicates that a high concentration of API is released initially, but the release level of the drug substance is relatively stable from one month to two years after insertion. Oncology implants are similar but have no outer shell. Ophthalmic implants are dramatically smaller in size and are very sensitive towards cutting. As such, the downstream equipment needs to be selected very carefully.

Good content uniformity and small tolerances in the dimensions of the implants are the most crucial factors to achieve controlled release of APIs in injectable implants. HME, including downstream equipment, is a flexible and reliable technology to compound the raw materials and manufacture injectable implants.

FIGURE 11: Example of a contraceptive implant.

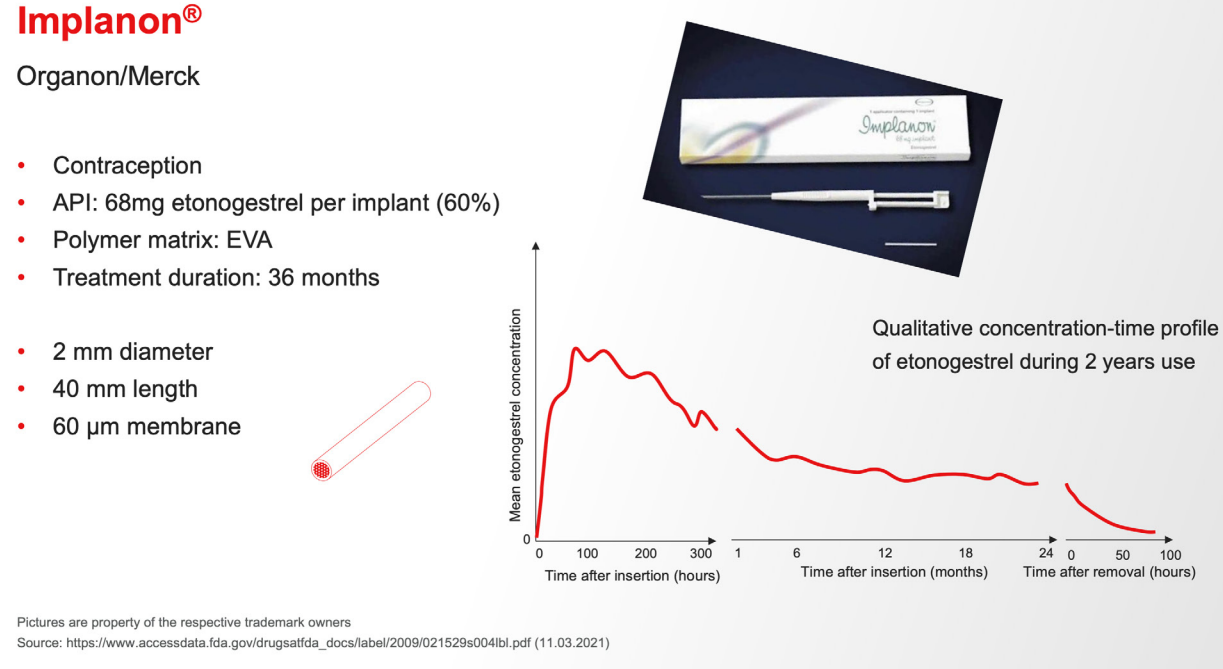

Pictures are property of the respective trademark owners
Source: https://www.accessdata.fda.gov/drugsatfda_docs/label/2009/021529s004lbl.pdf (11.03.2021)

Implants and Applications of Vibrational Spectroscopy

A myriad of applications of vibrational spectroscopy for the manufacture of coextruded drug implants, from raw-material verification, to PAT solutions, to final product QC are available. NIR and Raman are commonly utilized for coextrusion process monitoring. Shaileshkumar Karavadra highlighted a recent study that employed both techniques to gain a clear understanding of API concentration in a co-extruded pharmaceutical implant.

In the study, NIR and Raman models based on 70% to 130% API content were built and applied to in-line process control. **FIGURE 12** displays the API concentrations calculated with the Raman model. Red ovals show the transition in API content from 80% to 100% of the target value, blue stars show the transition from 100% to 120% of the target, and purple triangles show the transition in API content from 120% to 130% of the target value. The dispersion of the points in the graph reflects the relative inhomogeneity between implants, which was in accordance with the HPLC results.

This figure demonstrates that one can control the process during a batch production and thus, keep only implants with the appropriate percentage of API.

Raman hyperspectral imaging is extremely useful for determining API homogeneity and checking the integrity of the membrane in a co-extruded drug implant. To determine the shell thickness and its quality, Raman microscopy imaging was used. Possible defects of the layers could be easily determined as well as migration of the API from the inner

FIGURE 12: In-line process control: Raman.

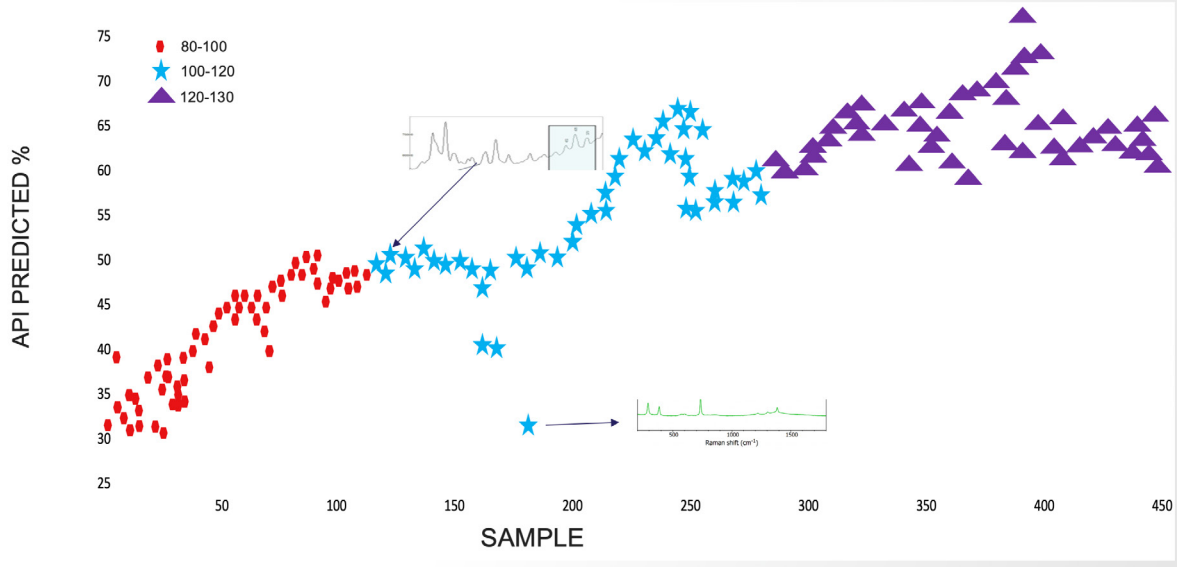

core to the outer shell. From the concentration maps, it was noted that the inner part of the implant contains homogenous API distribution. The integrity of the membrane is intact and there is no permeation of the API into the drug product. Thus, Raman microscopy enables visualization of the differences in the distribution of the domains in addition to the integrity of the membrane.

Raman 3D imaging is a very powerful tool that can be used to investigate multi-layer HME extrudates, such as transdermal patches. With no prior knowledge of the components, a nicotine patch was analyzed using confocal and Raman 3D imaging. Confocal microscopy observed four layers, while Raman 3D imaging utilizing MCR identified each layer and provided semi-quantitative data. Shown in **FIGURE 13**, spectra for the layers were consistent with nicotine, low density polyethylene, polyisobutylene, and polyethylene terephthalate (PET). This clearly demonstrates the benefit of using MCR for identification of an unknown sample and semi-quantitative analysis for the distribution of different domains. Raman 3D imaging can also identify and provide the location of contaminants and defects in multi-layered samples.

NIR and Raman spectroscopy have proven their utility for determining the API content within implants during the manufacturing process. Both techniques are fast and provide comparable results. In-line process measurement allows real-time control parameters such as extrudate diameter and API content. Raman hyper spectral imaging can be employed to control the blend homogeneity and the integrity of the membrane in co-extruded implants. Additionally, in-line, off-line (Raman imaging), and PAT tools provide deeper process understanding and can be integrated in a Real Time Release (RTR) or accelerated release strategy.

FIGURE 13: Nicotine patch Raman 3D imaging.

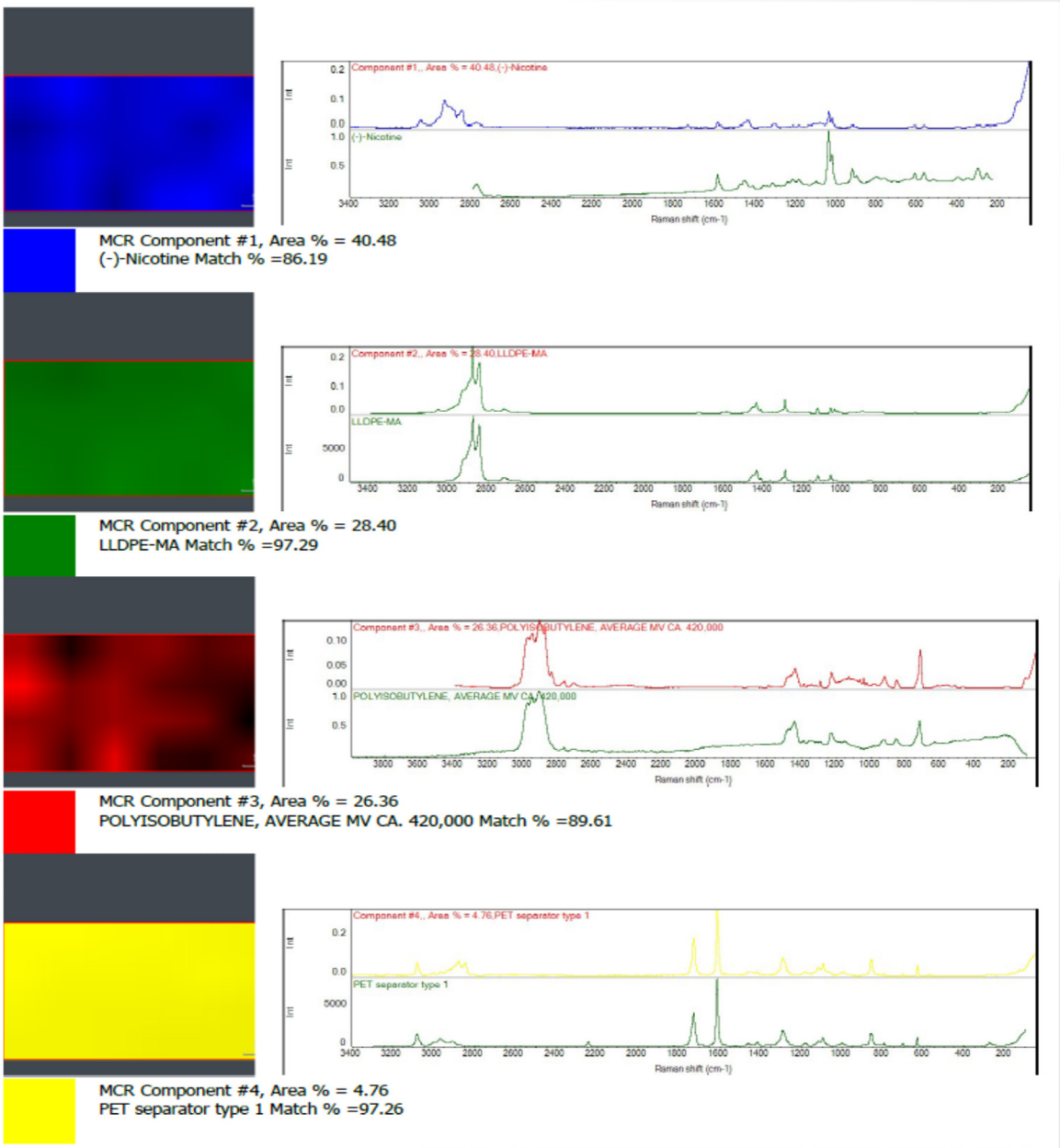

UV-VISIBLE SPECTROSCOPY FOR QUALITY CONTROL AND ADHERENCE TO PHARMACOPOEIAL STANDARDS

Identification of Color in Pharmaceutical Products According to Pharmacopeia Procedures

Dr. Jennifer Empey discussed how the color of a pharmaceutical product has implications in a variety of different aspects in the drug product development process. As both the USP and EP describe the necessary analytical methods for quantitatively determining the color of a drug product, UV-Visible absorption spectra of either liquids or powders are collected and used to determine the color values of the product.

In pharmaceutical sciences, identification of the specific color of a given drug product is particularly important in the quality assurance (QA) or quality control (QC) regime. The goals are to minimize any kind of batch-to-batch variations between products and identify any poor-quality products that may contain impurities or degradation. This can be particularly helpful to identify the dose based on the color of a product so that the colors are consistent within each dose. In trials, it is important to keep the color of placebos and drug products consistent with one other to eliminate unintentional bias. Color analysis is needed for both liquid and solid forms of drug products.

There are two general methods for color analysis: qualitative and quantitative. The qualitative or organoleptic method entails simply matching a standard and a sample with the naked eye by putting them next to each other and seeing if they match. Although this method requires no instrumentation, it is dependent upon the individual, thereby introducing inherent person-to-person variations. It is also highly dependent upon the environment for which the samples are analyzed, such as illumination/shadows or observer angle/field of view. Thus, while rapid, this method has the possibility of user error. A more rigorous, quantitative method uses instrumentation to provide a numeric value to the color of a sample. Using an instrument minimizes person-to-person variations and accounts for any environmental changes.

Humans perceive color through the collection of reflected light off an object by the eye. As human eyes are particularly sensitive photo detectors for visible light, they can perceive tiny differences in intensity and wavelengths of light that are reflected off a sample, allowing for the perception of small differences in color. As the color of an object is related to the reflected light, a light-based technique can be used to analyze color. As such, UV-Visible absorbance and reflectance spectroscopy can be used to analyze the samples and determine the color associated with the acquired spectra. Note that absorption and reflection are essentially inverses of one another. The Thermo Scientific™ Evolution™ One Plus Spectrophotometer is ideally suited to this application.

In trials, it is important to keep the color of placebos and drug products consistent with one other to eliminate unintentional bias.

Briefly, the basic concept of a UV-Vis absorption technique involves shining light on the samples with a specific intensity. It will interact with the sample and some of the photons will be absorbed so that a smaller intensity beam exits the sample and reaches the detector. This data is reported as the log of the ratio of the intensity of the initial light source to the intensity of the exiting light source. The ratio between these light sources is referred to as the transmission of the material, which can be related back to the absorbance. The acquired spectra report percent transmittance (%T) as a function of wavelength.

For opaque samples, such as powder or solid, the same instrument can be used in a slightly different optical geometry to measure the reflected intensity of light that bounces off the sample surface. In this case, the ratio between the intensity before and after the sample is irradiated is measured, similar to transmittance measurements. The acquired spectra report percent reflectance (%R) as a function of wavelength.

Although variations can be observed in spectra of different colored samples, it is difficult to assign a single numerical value for comparison between the samples and standards. Therefore, a more rigorous method is needed that provides a singular point to compare the color from sample to sample. Tristimulus values are a mathematical representation that places colors on an x,y,z coordinate system. This provides a single point in a color space for identification based on the reflected or transmitted spectrum. The calculation of tristimulus values incorporates the spectral power of the illuminant and a color-matching function, which are both dependent on the given application.

The illuminant is the light source under which the color of the object is to be determined. Different types of illuminants are specified for EP and USP pharmacopoeia compliance, such as D65 and C. Both represent the intensity of a daylight source. This illuminant should be selected based on the SOP or the monograph to be followed to ensure compliance. The observer angle is included in the color-matching function and defines the field of view at which the observer looks at an object. There are typically two observer angles recognized by USP and EP: 2 degrees and 10 degrees.

As the tristimulus color space is nonuniform, and consequently difficult for comparison between two samples, it is commonly transformed into a CIELAB color space (L*a*b*). Shown in **FIGURE 14**, L*a*b* sets the color on a spherical coordinate

FIGURE 14: CIELAB (L*a*b*).

$$L^* = 116\left(\frac{Y}{Y_n}\right)^{\frac{1}{3}} - 16$$

$$a^* = 500\left[\left(\frac{X}{X_n}\right)^{\frac{1}{3}} - \left(\frac{Y}{Y_n}\right)^{\frac{1}{3}}\right]$$

$$b^* = 200\left[\left(\frac{Y}{Y_n}\right)^{\frac{1}{3}} - \left(\frac{Z}{Z_n}\right)^{\frac{1}{3}}\right]$$

X_n, Y_n and Z_n are the color values of a white object assuming a perfectly reflecting diffuser

Compares sample CIELAB values to the values for a standard

Color Difference:

$$\Delta E^* = \sqrt{(\Delta L^*)^2 + (\Delta a^*)^2 + (\Delta b^*)^2}$$

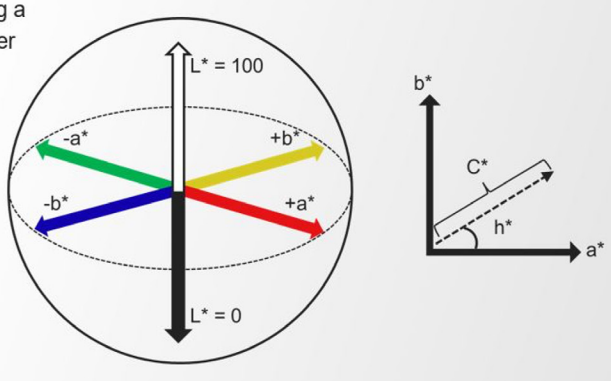

that allows for a better comparison between different samples and a standard. It essentially helps create a uniform space where all colors are referenced against a white object, considered a perfect diffuse reflector, allowing for normalization for any other measurement. In addition to generating the L*a*b* coordinates, a singular color difference value, ΔE*, can be calculated to compare the color of a sample with that of a given standard and pinpoint where the two are located in relation to one another on the spherical graph. Two other values are also shown on the L*a*b* diagram: hue and Chroma. L*C*h* values are commonly used in this color space to describe how colorful an object is (Chroma) or what that specific color is (hue). Note that EP allows using L*C*h* while the USP does not.

USP and EP procedures specify that if a quantitative method is employed, the spectrophotometer used for color analysis must be qualified according to their standards described in USP <857>.

USP and EP procedures specify that if a quantitative method is employed, the spectrophotometer used for color analysis must be qualified according to their standards described in USP <857>. The Thermo Scientific Evolution One, One Plus, and Pro performance specifications are USP and EP compliant. Typically, the measurement range covers 400 nm to 700 nm, spanning the visible region of the UV-visible spectrum. Both pharmacopoeia procedures call out using data intervals of 10 nm or less. Prior to measuring transmission samples, it is important to calibrate the instrument to determine what 0% transmittance (T) and 100% T spectra are for the instrument. The 0% T measurement involves blocking the beam with something that will prohibit any light from reaching the detector. To establish the 100% T baseline, purified water or a solvent that is relevant for the sample is measured. USP and EP call for specific illuminant and observer angles in chapter <631> and 2.2.2.2, respectively. It is important to note that turbid solutions must be filtered to avoid anomalous data from light scatter.

For the analysis of L*a*b* values, color matching solutions defined by USP specify the different proportions of a yellow (ferric chloride), red (cobalt chloride), and blue (copper sulfate) solution that must be mixed to produce a standard. USP recognizes the more stringent EP and Chinese pharmacopoeia matching solutions as well.

From USP <631>, multiple types of color analysis tests can be performed based on the requirements for the analyzed material. The first test assesses whether a solution is colorless (achromatic). Purified water is used as the standard for which a color difference is calculated. In this test, the spectra of water and the sample are both acquired, and the L*a*b* values are determined. The color difference value, ΔE*, is then calculated. ΔE* must be less than 1 to indicate that the solution is colorless, meaning that the color of the sample solution is indistinguishable from pure water.

A second method compares a sample to a given standard solution, which is useful for samples that are expected to have color; and that color must exactly match that of a standard. This method uses the same type of experiment and analysis as the achromaticity test, except a matching solution is to be used as the standard instead of purified water. In this case, the color difference value must be less than 3, as this is the theoretical limit at which the human eye can discern a change in color. If ΔE* is greater than 3, the eye should be capable of differentiating between the two.

Minimum and maximum color levels can also be specified when some variation in color is acceptable. A color standard is selected from the available USP and EP options, with a

hue from the L*C*h* space within 15 points of the sample. The color difference for the standard and samples are then tested against purified water. For the minimum color level, the ΔE* between the water and sample should be greater than the ΔE* between water and the standard. The converse is true for the maximum color level. Using this protocol, color difference measurements are being compared rather than comparing the color difference value with a specific value. Following these procedures enables the development of a variety of different experiments and limits that are important for samples of interest.

To demonstrate the application of color analysis to liquid samples, USP color-matching solutions were made according to USP procedure. Some of these color-matching solutions shown in **FIGURE 15** can be difficult to discern with the naked eye. However, transmission spectra and associated spherical coordinates in the L*a*b* space easily distinguish them from one another. Solutions that were particularly difficult to differentiate by eye are highlighted with boxes in the photo and listed in the table. L*a*b* values in the table for each pair are fairly close to one another. However, the last column shows the color difference analysis results (ΔE*). Since all values are greater than 3, the pairs do not pass the matching test and are considered distinguishable from one another. Although the differences in color were nearly imperceptible to the naked eye, the instrumentation was able to easily discern them.

A more realistic example of a liquid sample is shown in **FIGURE 16**, for which the colors of day-time and night-time cough syrups were compared. Initially, an absorption spectrum was collected in a standard 10 mm path. The spectrum shows high absorption from 400 nm to 600 nm, and the L*a*b* graph indicates that the day-time cough syrup was nearly out of bounds, as it absorbed too much in the yellow region. Beer's Law states that absorbance and path length are directly proportional, so decreasing the path

FIGURE 15: USP color matching solutions.

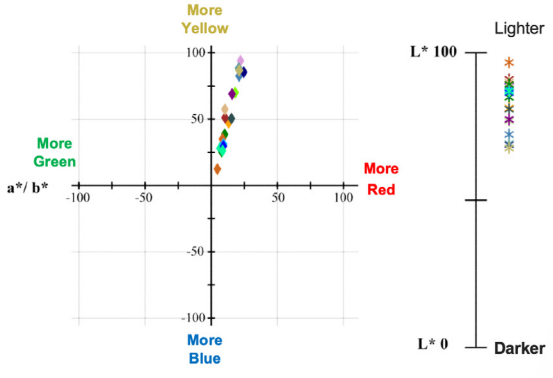

Illuminant = D65
Observer Angle = 10°

Standard Solution	L*	a*	b*	ΔE*
A	87.5	0.5	28.5	9.7
B	83.3	2.4	37.0	
J	69.1	12.0	80.0	12.5
K	73.9	12.5	91.5	
Q	85.1	2.6	28.3	5.2
R	88.1	2.5	24.0	

ΔE* > 3

Do not pass as discernable

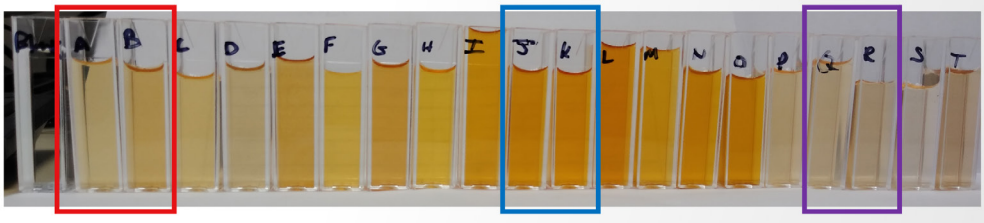

FIGURE 16: Highly absorbing samples: cough syrup.

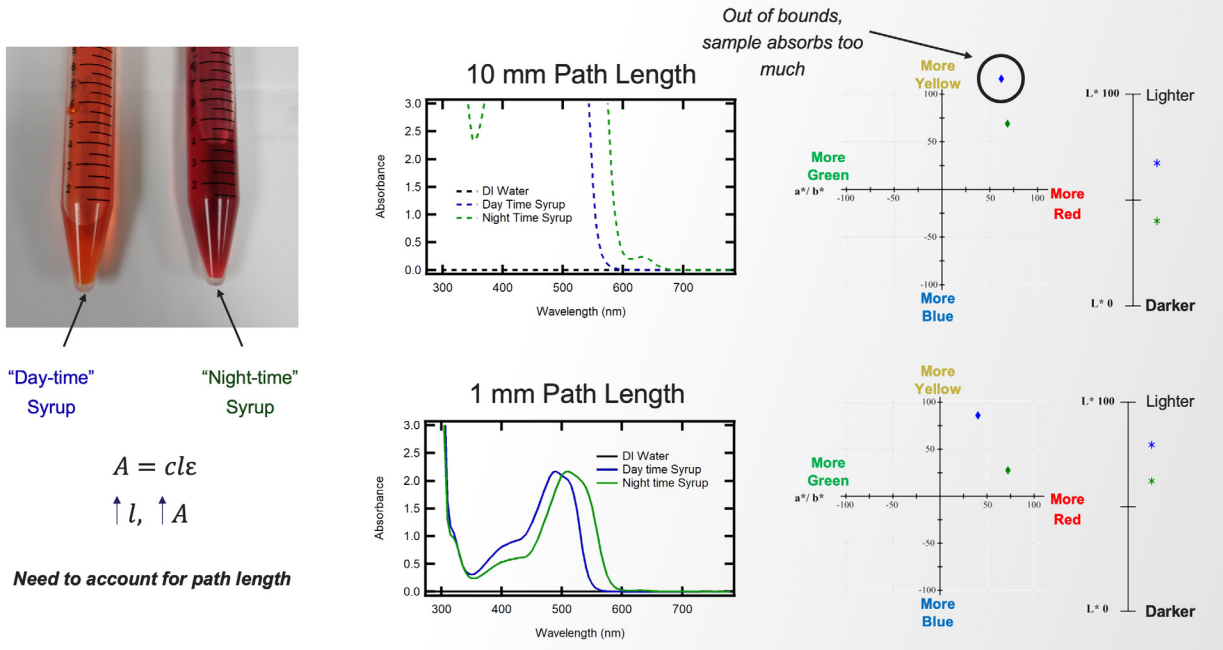

length will decrease the measured absorbance of a material. A subsequent data collection used a 1 mm path length to acquire a more discernible absorption spectrum as well as more reliable L*a*b* values, as shown at the bottom of the figure. This example illustrates the importance of considering absorbance and path length for the measurements.

Solid samples cannot be easily measured with transmission measurements, as it is difficult to pass light through the material. However, reflectance measurements are possible and can be used for color analysis. This analysis requires a reflective accessory, such as the Thermo Scientific™ ISA-220 Integrating Sphere Accessory, for the Evolution One Plus Spectrophotometer. To demonstrate this technique, the CIELAB color values of four antacid tablets was determined using the Evolution One Plus system and ISA-220 accessory. An integrating sphere can either collect diffusely reflected light only or "total" reflections (diffuse plus specular reflections) to produce a reflectance spectrum without scattering artifacts. For non-glossy solids, such as powders or tablets which reflect mostly diffuse light, the ISA can be a very useful analysis tool. As demonstrated in **FIGURE 17**, the antacid samples studied (Tablets A-D) appear by eye to be white, yellow, orange and red, respectively. Variations between the collected reflectance spectra were observed and the color difference was calculated against a white reflectance standard for each tablet. As expected, the color difference for Tablets B, C, and D were well above 3, indicating they are distinguishable from the white standard. Upon comparison to Tablet A, the ΔE* was also found to be outside of the acceptance criteria (ΔE* < 3), indicating the color of Tablet A is also distinguishable from the white reflectance standard. Though by eye Tablet A appeared similar in color to the white standard, the instrumentation was able to distinguish the color between the two materials.

These examples demonstrate the power of quantitative color analysis through UV-Visible spectroscopy, proving to be a much more effective technique than color matching by eye. This analysis can be applied not only to solutions through transmission measurements, but

FIGURE 17: Observations of the CIELAB color values of four antacid tablets using the Evolution One Plus and ISA-220.

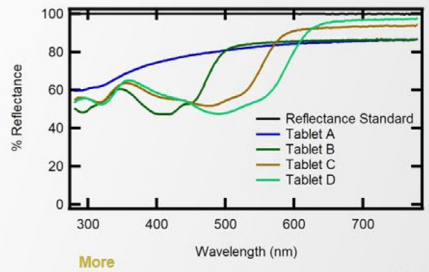

To Pass: ΔE*<3

Illuminant = D65
Observer Angle = 10°

Tablet	L*	a*	b*	ΔE* (referenced against standard)
A	92.8	0.3	3.4	8.0
B	92.8	-5.8	21.7	23.6
C	88.1	13.7	17.0	24.9
D	82.5	19.3	8.7	27.5

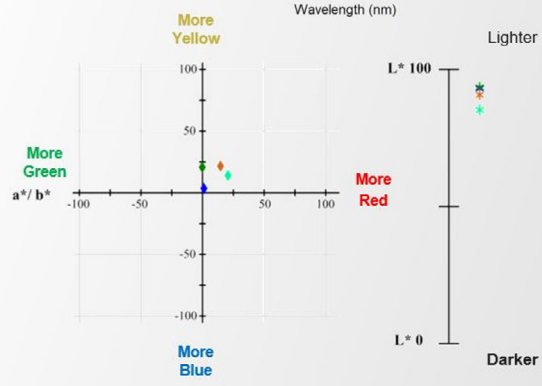

also to solid samples through reflectance measurements. Additionally, the mathematics behind the technique allow for a rigorous comparison against given standards. The calculated results can be reported in values required for pharmacopeial compliance. Perfectly suited for color analysis, Evolution One, One Plus, and Pro Spectrophotometer performance specifications are USP and EP compliant and use software that enables the ability to report the required color analysis calculations, including CIELAB, L*C*h* and color difference values.

CONCLUSION

Optimization of drug formulation, delivery, production, and downstream processing are critical aspects of the pharmaceutical domain. In support of these steps, reliable in-line and off-line analytical technologies ensure consistent, high-quality products. In addition to a suite of robust hot-melt extruders and accessories for pharmaceutical production and processing, Thermo Fisher Scientific offers a vast array of analytical instrumentation to drive deeper materials insights. With state-of-the-art solutions for spectroscopy and microanalysis, as well as advanced software, users can quickly go from questions to usable data. The company's full spectrum of high-performance analytical tools enables pharmaceutical companies to push the boundaries of productivity and innovation.

REFERENCES

1. M. Leane, K. Pitt, and G. Reynolds. *Pharm Dev Technol*. **20** 12-21 (2015).
2. C.K. Tye, C.C. Sun, and G.E. Amidon. *Journal of Pharmaceutical Sciences*. **94** (3) 465-72 (2005).